Influence of Chirp of High-Speed Laser Diodes and Fiber Dispersion on Performance of Non-Amplified 40-Gbps Optical Fiber Links

Moustafa Ahmed, Ahmed Bakry, Safwat W. Z. Mahmoud

Abstract—We model and simulate the combined effect of fiber dispersion and frequency chirp of a directly modulated high-speed laser diode on the figures of merit of a non-amplified 40-Gbps optical fiber link. We consider both the return to zero (RZ) and non-return to zero (NRZ) patterns of the pseudorandom modulation bits. The performance of the fiber communication system is assessed by the fiber-length limitation due to the fiber dispersion. We study the influence of replacing standard single-mode fibers by non-zero dispersion-shifted fibers on the maximum fiber length and evaluate the associated power penalty. We introduce new dispersion tolerances for 1-dB power penalty of the RZ and NRZ 40-Gbps optical fiber links.

Keywords—Bit error rate, dispersion, frequency chirp, fiber communications, semiconductor laser.

I. INTRODUCTION

IN the current information age, there is a steady need to increase the capacity of information transmitted to or exchanged among users, especially over optical fibers. Modern cost-effective and broadband fiber networks, such as the fiber-to-the-home (FTTH) and radio over fiber (RoF), require directly modulated laser diodes with bandwidth exceeding 25 GHz for operating the fiber links with transmission speeds exceeding 40 Gbps [1]. Due to the inferior characteristics in the transient regime of the semiconductor laser, its resonance and modulation bandwidth are limited to values more or less than 10 GHz. One typical solution to increase the modulation bandwidth is to increase the differential gain of the laser diode [2], [3]. This property is a typical advantage of the MQW laser diodes [4]. Sato et al. [3] demonstrated a MQW-DFB laser emitting at the wavelength of 1.55 μm to meet the requirement of 40 Gbps fiber transmission systems for use in very-short-reach fiber links and metro area networks [5].

The intensity modulation of high-speed semiconductor lasers, however, is coupled to the phase variation through the linewidth enhancement factor [6], [7] which then induces a time variation in the lasing frequency, referred to as "frequency chirp" [8]. This frequency chirp is proportional to the differential gain and, therefore, attains large in high-speed

M. Ahmed and A. Bakry are with the Department of Physics, Faculty of Science, King Abdulaziz University, 80203 Jeddah 21589, Saudi Arabia (phone: +966-53-4094194; fax: +966-12-6064277; e-mail: mostafa.hafez@science.miniauniv.edu.eg, abakry@kau.edu.sa).

S. W. Z. Mahmoud iswith the Department of Physics, Faculty of Science, Minia University, 61519 Minia, Egypt (e-mail: safwatwilliam@yahoo.com).

laser diodes [9]. The frequency chirp was proved to interact with fiber dispersion in such a way to degrade performance of fiber communication systems [9]-[15]. Forms of this performance degradation include limitations to the transmission bit rate, transmission distance, and addition to the power penalty of the fiber system [16], [17]. Fiber communication systems operating at the wavelength of 1.55 μm have fiber dispersion as high as 16.75 ps/nm-km, which enhances the effect of the laser chirp [8]. One technique to reduce such an effect is to replace SSMFs by DSFs in which the fiber dispersion is shifted to either long or short sides of the lasing wavelength [8], [16]. It is then necessary to investigate the combined effect of the laser chirp and fiber dispersion on the performance of directly-modulated 40 Gbps fiber links using both SSMFs and DSFs. On the other hand, most previous studies spotted on the laser behavior under NRZ modulation, whereas a few reports compared the modulation characteristics under the RZ and NRZ bit patterns [18]-[22].

In this paper, we simulate the characteristics of 40-Gbps fiber communication systems utilizing high speed quantum-well 1.55-μm DFB laser diodes. The fiber system is designed and simulated using the Optisystem software. We quantify the performance of the fiber system in terms of the characteristic relation between the bit error rate (BER) and the received power. Limitations on the fiber length due to the combined effect of the laser chirp and fiber dispersion is also examined. In additions, we quantify the improvement of the fiber system performance by replacing SSMFs by NZ-DSFs and calculate the associated power penalty. We show that this power penalty is enhanced in the vicinity of zero dispersion, while it drops too much at other dispersion values. The RZ-pattern induces power penalty due to this dispersion variation higher than the NRZ pattern. New dispersion tolerances are explored for 1-dB power penalty of the RZ and NRZ optical fiber links.

II. SIMULATION MODEL OF FIBER COMMUNICATION SYSTEM

The proposed fiber communication system deploying a high speed semiconductor laser is sketched in Fig. 1. The data sequence with bit rate $B = 40$ Gb/s is generated by a $2^{10}-1$ pseudo-random bit sequence (PRBS) generator. This information code is then converted into electrical signals with either RZ or NRZ formats using a pulse generator. In the laser driver model, the bias and modulation currents are combined (direct modulation), and the output current waveform is recorded. The laser signal is transmitted down a standard

single-mode fiber with an average output power P_T. The fiber has length L_f, attenuation coefficient α_f, and dispersion D, and group velocity dispersion (GVD) which is responsible for the pulse broadening. The optical field is assumed to maintain its polarization along the fiber length. At the receiver, the laser signal is detected and converted into an electrical signal $i(t)$ by a PIN photodetector. Both the shot noise and thermal noise are taken into account and are assumed to have Gaussian statistics [9]. The corresponding errors in identification of the "1" and "0" bits are evaluated in terms of BER. The high-speed fiber system is designed and simulated by the Optisystem software. Details on the theoretical model of simulating the fiber system components can be found in [24]

The parameters of the fiber system components and their numerical values used in the Optisystem software are listed in Table I [3]. The modulation bit rate is set to be B = 40 G/ps, which corresponds to bit slot $T_b = 1/B = 25ps$. The duty cycle of the RZ bits is set to be 0.5. The proposed laser diode is a strained MQW-DFB 1.55-μm InGaAsP laser [3]. The calculated threshold current is I_{th}=9.84mA. The bias and modulation currents are set to be I_b=92 mA and I_{PK}=90 mA, respectively. Basing on the small-signal modulation analysis [9], [25], these currents correspond to a modulation bandwidth frequency of 28 GHz, which agrees with the values measured by Sato et al. [3]. Biasing the laser above threshold is necessary to realize long-span transmission systems because this results in decreasing the spectral spread of the directly modulated laser, increasing the extinction ratio for the transmitted optical signal, and improving the receiver sensitivity [26]. The corresponding launched power to the optical fiber is $\overline{P_{tr}} = 11 dBm$ .The proposed PIN photodetector is used with a low-pass Bessel filter of order four [8]. Parameters of the power budget of the fiber system, including the power margin, and connection and splice losses are also listed in Table I [8].

III. RESULTS AND DISCUSSION

The high-speed laser considered in this paper was proved to peak-to-peak chirps of 65.1 and 77.8 GHz when it is modulated by the RZ and NRZ bit codes with bit rate of 40 GHz. In this section, we examine influence of fiber dispersion on the performance of the 40 Gbps fiber communication system with such large frequency chirp. The parameters of the performance evaluation include the eye diagram of the detected signal, receiver sensitivity, attenuation-limited fiber length, and dispersion-limited fiber length. The power penalties due to fiber dispersion and laser chirp are also evaluated. Table II summarizes the obtained results of these performance evaluation parameters.
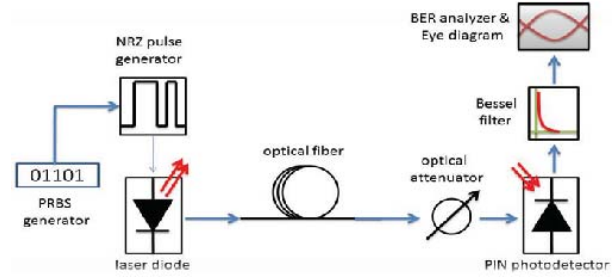

Fig. 1 Scheme of the designed fiber communication system

TABLE I
PARAMETERIC VALUES OF THE PROPOSED OPTICAL FIBER COMMUNICATION SYSTEM [3], [8]

Symbol	Quantity	Value
Laser diode		
λ	Wavelength	1.55 μm
V	Active layer volume	3×10^{-11} cm^3
v_g	Group velocity	8.33×10^9 cm/s
η_0	Quantum efficiency	0.255
A_0	Differential gain coefficient	9.9×10^{-16} cm^2
N_g	Carrier density at transparency	1.23×10^{18} cm^{-3}
α	Linewidth enhancement factor	3.5
Γ	Mode confinement factor	0.2
A_{nr}	Recombination coefficient	10^8 s^{-1}
B_r	Recombination coefficient	3.5×10^{-10} cm^3/s
C_{AUG}	Recombination coefficient	7.5×10^{-29} cm^6/s
τ_p	Photon lifetime	1.69×10^{-12} s
β_{sp}	Spontaneous emission factor	3×10^{-5}
ε	Gain compression coefficient	2.77×10^{-17} cm^3
PIN Photodetector		
R	Responsivity	1 A/W
I_{th}	Thermal noise	10^{-22} W/Hz
I_d	Dark current	10 nA
Optical fiber		
α	Attenuation coefficient	0.18 dB/km
D	Dispersion	16.75 ps/nm/km
S	Dispersion slope	0.075 ps/nm^2/km
β_2	Dispersion parameter	-20 ps^2/km
System Parameters		
M_S	System Margin	4.5 dB
α_{con}	Connection loss	1 dB
α_{splice}	Splice loss	0.5dB

TABLE II
OBTAINED VALUES OF THE PERFORMANCE EVALUATION PARAMETERS OF THE PROPOSED FIBER SYSTEM

Parameter	RZ	NRZ
Transient chirp $\Delta \nu$ (GHz)	65.1	72.8
Receiver sensitivity R_S (dBm)	-3.29	-4.21
Attenuation-limited fiber length L_{F-attn} (km)	37.4	46.1
Dispersion-limited fiber length L_{F-disp} (km)	2.51	1.37

A. Eye Diagram and Receiver Sensitivity

The receiver sensitivity R_S is determined as the minimum received power P_{rec} required to achieve BER of 10^{-9}. It is determined using the back-to-back configuration in which the laser signal is attenuated by means of a power attenuator and then strikes the PIN photodiode. BER is then calculated at each value of the attenuated power P_{rec}. The simulated

characteristic (BER versus P_{rec}) curves for the RZ and NRZ bit formats are plotted in Fig. 2 (a). The figure shows that BER drops to lower orders of magnitude with the decrease in P_{rec} due to increase in the on-off ratio [25]. The slope of this drop of BER is smaller under the RZ modulation than that under the NRZ modulation, which manifests as an increase in the relevant range of P_{rec}. Fig. 2 (a) indicates that the obtained results of the receiver sensitivity are R_S = -4.21 and -3.29 dBm under the NRZ and RZ modulations, respectively. That is, the NRZ-modulated signal requires power higher than that required by the NRZ-modulated signal to maintain the same range of BER. In other words, the NRZ modulation corresponds to better performance in the back-to-back configuration of the system.
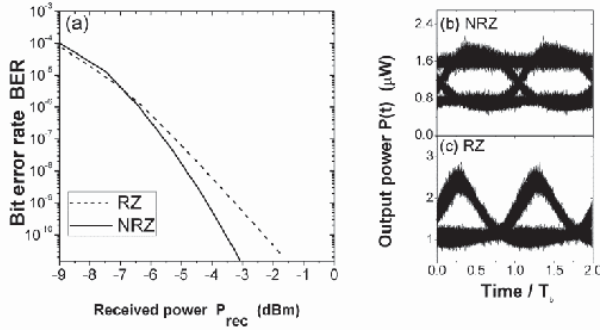

Fig. 2 (a) BER versus received power P_{rec}, and the simulated eye diagrams under (b) NRZ modulation and (c) RZ modulation when BER = 10^{-9}

The eye diagrams of the NRZ and RZ-modulated signals at the boundary of BER=10^{-9} are plotted in Figs. 2 (b) and (c), respectively. The eye diagram is a conventional and visual tool to monitor the complete waveform of the modulated laser signal. Each eye diagram is constructed by cutting the waveform of the laser signal into 2-bit segments and plotting each segment onto others. The figures show that the eye diagrams are open at this level of received power P_{rec}. The thick horizontal borders of both the "1" and "0" levels of the eye diagrams are manifestation of laser and receiver noises. The budge on top of the eye diagrams are due to the bit-pattern effect raised because the bit slot T_b is shorter than the setting time of the relaxation oscillations [22], [23]. This bit-pattern effect is also the origin of the random rising and falling paths between the "0" and "1" levels and the associated turn-on and turn-off jitters [23].

B. Influence of Fiber Attenuation

Due to fiber attenuation, an upper limit is set to the fiber length. This maximum fiber length is known as "attenuation-limited fiber length", L_{f-attn}, and is predicted from the power budget equation of the system [8]:

$$L_{f-attn} = \frac{\overline{P}_{tr} - S_R - \alpha_{con} - \alpha_{splice} - M_s}{\alpha_f} \qquad (1)$$

where α_f is the attenuation coefficient of the fiber, and α_{con} and α_{splice} are fiber losses due to connections and splicing, respectively. The calculated values of L_{f-attn} under the NRZ and RZ bit patterns are 45.8 and 37.3 km, respectively. That is, the maximum fiber length is larger under the NRZ bit pattern than that under the RZ bit pattern. The obtained values of this fiber length L_{f-attn} are comparable to the values of 46.1 and 37.4 km.
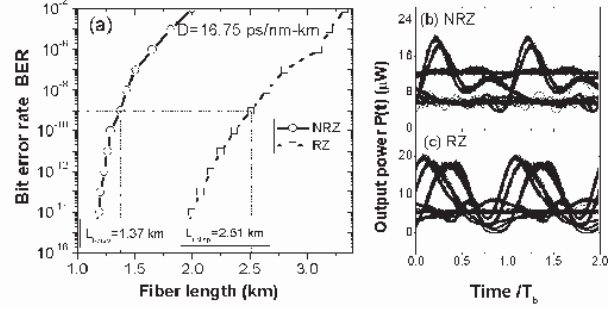

Fig. 3 BER versus fiber length L_F with fiber dispersion, (a), and the simulated eye diagrams under (b) NRZ modulation and (c) RZ modulation. The maximum fiber length L_{F-disp} corresponds to BER = 10^{-9}

C. Influence of Fiber Dispersion

Although the laser diode is assumed to oscillate in single mode, it has nonzero linewidth or finite chirp [27]. Therefore, the fiber chromatic dispersion should cause broadening of the signal transmitted down the fiber and adds more limitation to the fiber length [8], [24]. The dispersion-limited fiber length is evaluated as follows. The fiber dispersion is ignored and the fiber length is varied over a wide range. At each fiber length, the eye diagram is monitored and BER is evaluated. Then L_{f-attn} is decided as the fiber length at which BER=10^{-9}. Fig. 3 (a) plots the variation of BER with fiber length L_f, showing that L_{f-disp} is limited to the values of L_{f-disp} = 1.37 and 2.51 km under the NRZ and RZ bit patterns, respectively, which are much shorter than the attenuation limited fiber lengths. By recalling that the chirp under the RZ modulation, Δf = 65.1 GHz, is lower than that, Δf = 77.8 GHz, under the NRZ modulation, we conclude that the frequency chirp is a main contributor to this limitation of the fiber length. This result enhances the effect of the frequency chirp as a main degrading factor to the performance of the directly-modulated high-speed fiber systems. The obtained values of L_{f-disp} are much larger than the value of 60 km predicted by Ahmed [24] using conventional laser diodes with chirp of $\Delta f \sim$ 19 GHz, and by Kim et al. [28] and Tomkos et al. [29] at B = 10 Gbps. Figs. 5 (b) and (c) plot the eye diagrams at the values of L_{f-disp} under the NRZ and RZ bit patterns, respectively. The eye diagrams exhibit resolved paths to rise to the "1" level or to fall to the "0" level, which are due to the pseudorandom bit pattern effect [21]. These results indicate that the combined effect of fiber dispersion and frequency chirp of the laser on the transmitted laser signal is influenced by the pseudorandom bit pattern effect, depending on the history of the "0" bits preceding each "0" bit.
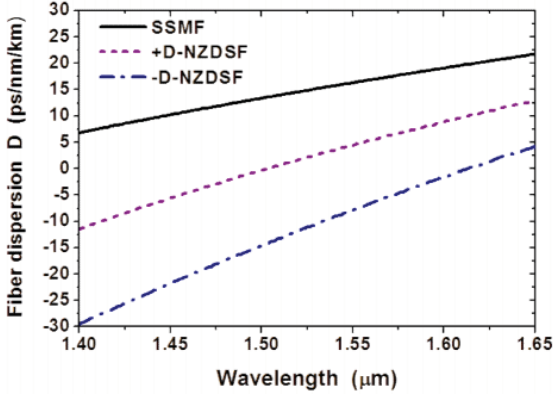
Fig. 4 Variation of fiber dispersion D with wavelength for both SSMFs and positive NZ-DSFs or negative NZ-DSFs
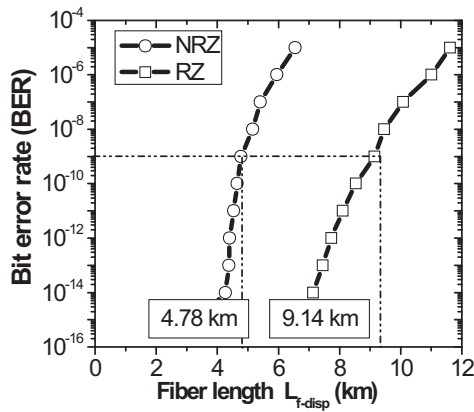

Fig. 5 BER versus fiber length L_f using NZ-DSFs with D = +4.5 ps/nm/km under the NRZ and RZ bit patterns. The maximum fiber length $L_{f\text{-}disp}$ corresponds to BER = 10^{-9}.
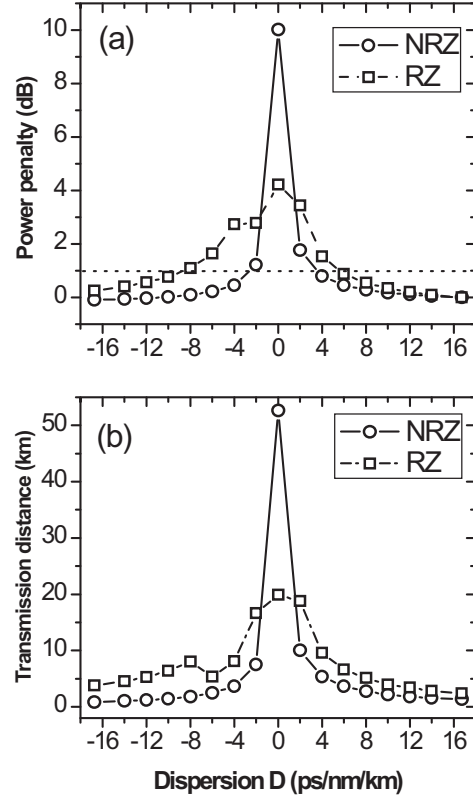

Fig. 6 Influence of varying the fiber dispersion by using NZ-DSF on (a) the power penalty of the 40-Gbps fiber system and (b) the dispersion-limited fiber length $L_{f\text{-}disp}$ under NRZ and RZ modulation bit patterns

D. System Performance Using NZ-DSFs

The idea of using the NZ-DSF is illustrated in Fig. 4 in which the single-mode fiber can be replaced by a positive NZ-SDF or a negative NZ-SDF. This variation of fiber dispersion may work against the laser chirp and improve the system performance. An example illustrating the performance of the fiber system using the positive NZ-SDF is given in Fig. 5 in which the dispersion parameter D is reduced to 4.5 ps/nm/km. The figure plots variation of BER with fiber length L_f, and shows that the dispersion-limited fiber $L_{f\text{-}disp}$ improves to 9.14 and 4.78 km under the RZ and NRZ bit patterns, respectively. That is, the positive NZ-SDF improves the fiber length to be suitable for use these links in short-reach optical fiber links.

Replacement of the SSMFs with D = 16.75 ps/nm/km by NZ-DSFs is associated with a variation in the received power required to maintain BER at 10^{-9}. That is, power penalty is induced and the fiber length is changed. We evaluate the power penalty associated with the variation of D from the value of D = 16.75 ps/nm/km according to the relationship

$$Power\ penalty\ (dB) = 10\log\frac{P_{rec}(D)}{P_{rec}(D = 16.75\ ps/nm/km)} \quad (2)$$

The calculated values of the power penalty as a function of the fiber dispersion D are plotted in Fig. 6 (a) in which D is varied between −25 and +25 ps/nm/km. The corresponding variation in the dispersion-limited fiber length $L_{f\text{-}disp}$ is plotted in Fig. 6 (b). Fig. 6 (a) indicates that the power penalty is too much enhanced around D = 0 (back to back configuration), and the NRZ modulation reveals higher power penalties than the RZ modulation. Apart from vicinity of D = 0, the power penalty associated with shifting the fiber dispersion is higher under the RZ bit pattern than under the NRZ bit pattern. Fig. 6 (b) indicates that the maximum fiber length $L_{f\text{-}disp}$ changes with D in a similar fashion to the power penalty. $L_{f\text{-}disp}$ reaches the maximum values of 53 km when D = 0 around which the NRZ modulation results in longer fiber lengths than those under the RZ modulation. When $|D|$ exceeds 2 ps/nm/km, the performance of the RZ modulation becomes better than that of the NRZ modulation, and the maximum fiber length is limited to $L_{f\text{-}disp}$ = 10 km.

We use the variation in the power penalty with the fiber dispersion to setup a dispersion tolerance to the simulated fiber communication system. We assign to this dispersion penalty the values of the dispersion coefficient D that yield power penalty within 1 dB. The figure indicates that the dispersion tolerance is $-4\,ps/nm/km \leq D \leq -2\,ps/nm/kn$ under the

NRZ modulation, whereas it is $-4\,\text{ps/nm/km} \le D \le 6\,\text{ps/nm/km}$ under the RZ modulation. Fig. 6 (b) shows that within this dispersion tolerance, the limited fiber length $L_{f\text{-}disp}$ ranges between 4 and 8 km under the RZ bit pattern and between 1 and 6 km under the NRZ bit pattern.

IV. CONCLUSION

We studied the influence of both the fiber dispersion and the frequency chirp of high-speed MQW laser diodes on the performance of 40-Gbps optical fiber links. The system performance is evaluated in terms of eye diagram, receiver sensitivity, and limitation on the maximum fiber length. The results showed that the laser chirp is combined with the fiber dispersion in such a way to limit the fiber length to 2.51 and 1.37 km under the RZ and NRZ formats, respectively. This combination effect is influenced by the pseudorandom bit pattern effect depending on the history of the "0" bits preceding each "0" bit. Replacement of the SSMF by NZ-DSFs is associated with power penalty, which is too much enhanced around $D = 0$, and the NRZ modulation revealed power penalties higher than the RZ modulation. Apart from vicinity of this dispersion less fiber, the power penalty associated with shifting the fiber dispersion is higher under the RZ pattern than under the NRZ pattern. By defining dispersion tolerance to the values of D that yield power penalty within 1 dB, we report on the new dispersion tolerance of $-4\,\text{ps/nm/km} \le D \le 6\,\text{ps/nm/km}$ for the RZ modulated fiber communication systems and $-2\,\text{ps/nm/km} \le D \le 4\,\text{ps/nm/km}$ for the NRZ modulated-systems. Within this dispersion tolerance, the limited fiber length $L_{f\text{-}disp}$ ranges between 4 and 8 km under the RZ bit pattern and between 1 and 6 km under the NRZ bit pattern.

REFERENCES

[1] H. Dalir and F. Koyama, "Bandwidth enhancement of single-mode VCSEL with lateral optical feedback of slow light," *IEICE Electron. Express*, vol. 8, July 2011, pp. 1075–1081.
[2] K. Petermann, *Laser diode modulation and noise*. Kluwer Academic Publishers, Dordrecht, 1988.
[3] K. Sato, S. Kuwahar, and Y. Miyamoto, "Chirp characteristics of 40-Gb/s directly modulated distributed-feedback laser diodes," *J. Lightwave Technol.*, vol. 23, Nov. 2005, pp. 3790-3797.
[4] K. Yvind, D. Larsson, L. J. Christiansen, C. Angelo, L. K. Oxenlowe, J. Mork, D. Birkedal, J. M. Hvan, and J. Hanberg, "Low-jitter and high-power 40-GHz all-active mode-locked lasers," *IEEE Photon. Technno.Lett.,*vol. 16, April 2004, pp. 975-977.
[5] ITU-T draft recommendation G. 693, "Optical interfaces for intra-office systems," 2001.
[6] C. H. Henry, "Phase noise in injection lasers," *IEEE J. Lightwave Technol.*, vol. LT-4, March 1986, pp. 298–311.
[7] M. Ahmed, "Spectral lineshape and noise of semiconductor lasers under analog intensity modulation," *J. Phys. D.*, vol. 41, Aug. 2008, 175104 (10pp).
[8] G. P. Agrawal, *Fiber-optic communication systems*. John Wiley & Sons Inc., New York , 2002.
[9] M. F. Ahmed, A. H. Bakry and F. T. Albelady, "Digital Modulation Characteristics of High-Speed Semiconductor Laser for Use in Optical Communication Systems," Arab. J. Sci. Eng., vol. 39, April 2014, pp. 5745 – 5752.
[10] T. L. Koch, and J. E. Bowers, "Nature of wavelength chirping in directly modulated semiconductor lasers," *Electron. Lett.,* vol. 20, Dec. 1984, pp. 1038 -1039.
[11] K. Y. Lau, "Gain switching of semiconductor injection lasers," *J.Appl Phys. Lett.,* vol. 52, Jan. 1988, pp. 257-259.
[12] H. F. Liu, S. Oshiba, Y. Ogawa and Y. Kawai, "Method of Generating Nearly Transform-Limited Pulses from Gain-Switched Distributed-Feedback Laser Diodes and Its Application to Soliton Transmission", *Opt. Lett.*, vol. 17, Jan. 1992, pp. 64 – 66.
[13] E. Peral, W. K. Marshall, and A. Yariv, "Precise measurement of semiconductor laser chirp using effect of propagation in dispersive fiber and application to simulation of transmission through fiber gratings," *J. Lightwave Technol.,* vol. 16, Oct. 1998, pp. 1874-1880.
[14] A. Villafranca, J. Lasobras, and I. Garcés, "Precise characterization of the frequency chirp in directly modulated DFB laser," Prec. 6th Spa. Conf. Electron. Dev. Madrid, 2007, pp. 173 - 176.
[15] O. Boukari, L.Hassine, O.Latry, M. Ketata, and H. Bouchriha. "Characterization of the chirp in semiconductor laser under modulation," *J. Mat. Sci. Eng. C*, vol. 28, July 2009, pp. 671–675.
[16] P. Krehlik "Directly modulated lasers in negative dispersion fiber links," *Opto-Electron. Rev.*, vol. 15, June 2007, pp 71-77.
[17] M. Ahmed, "Modeling and simulation of dispersion-limited fiber communication systems employing directly modulated laser diodes," *Indian J. Phys.,* vol. 86, Nov. 2012, pp. 1013-1020.
[18] S. Balle, M. Homar, and M. S. Miguel, "Statistical properties of the spectrum of light pulses in fast pseudorandom word modulation of a single-mode semiconductor laser," *IEEE J. Quantum Electron.,* vol. 31, Aug. 1995, pp. 1401-1408.
[19] A. Yin, L. Li, and X. Zhang, "Analysis of modulation format in the 40 Gbit/s optical communication system," *Optik - Intl. J. Light and Electron. Opt.,* vol. 121, Sept. 2010, pp. 1550-1557.
[20] D. Liu, L. Wang, and J.-J. He, "Rate equation analysis of high speed Q-modulated semiconductor laser," *J. Lightwave Technol.,* vol. 28, Sept. 2010, pp. 3128-3135.
[21] M. Ahmed, S. Mahmoud, and A. Mahmoud, "Influence of pseudorandom bit format on the direct modulation performance of semiconductor lasers," *Pramana J. Phys.,* vol. 79, Dec. 2012, pp. 1443-1456.
[22] M. Ahmed, S. W. Z. Mahmoud, and A. A. Mahmoud, "Comparative study on modulation dynamic characteristics of laser diodes using RZ and NRZ bit formats," *Int. J. of Num. Model.*, vol. 27, May 2013, pp. 138-152.
[23] M. Ahmed, M. Yamada, and S. W. Z. Mahmoud, "Analysis of semiconductor laser dynamics under gigabit rate modulation," *J. Appl. Phys.*, vol. 101 , Feb. 2007, pp. 3119-3126.
[24] M. Ahmed, "Influence of transmission bit rate on performance of optical fiber communication systems with direct modulation of laser diodes," J. Phys. D, vol. 42, Sept. 2009, pp. 185104-185111.
[25] M. Ahmed and A. El-Lafi, "Analysis of small-signal intensity modulation of semiconductor lasers taking account of gain suppression," *Pramana J. Phys.***,** vol. 71, July 2008, pp.99-115.
[26] S. W. Z. Mahmoud, M. Ahmed, and R. Michalzik, "Influence of optical feedback-induced phase on turn-on dynamics of vertical-cavity surface-emitting lasers," Proc. 46th IEEE Midwest Symp. Circuit. Syst. (MWSCAS'2003), Cairo, Dec. 2004, pp. 1354-1358.
[27] M. Ahmed, "Numerical approach to field fluctuations and spectral lineshape in InGaAsP laser diodes", *Intl. J. Numer. Model.Simul.*Vol. 17, March 2004, pp. 147-163.
[28] I. Kim, T. J. Miller, and Y. K. Park, "10-Gb/s transmission using 1.3-μm low-chirp high-power directly modulated, packaged DFB laser module for short distance (<50 km) applications," *IEEE Photon. Technol. Lett. ,* vol. 9, Aug. 1997, pp. 1167-1169.
[29] I. Tomkos, B. Hallock, I. Roudas, R. Hesse, A. Boskovic, J. Nakano, and R. Vodhanel, "10-Gb/s transmission of 1.55-μm directly modulated signal over 100 km of negative dispersion fiber," *IEEE Photon. Technol. Lett.,* vol. 13, Jul. 2001, pp. 735-737.